Progress In Electromagnetics Research, PIER 28, 29–42, 2000

NEAR-FIELD AND FAR-FIELD EXPANSIONS FOR TRAVELING-WAVE CIRCULAR LOOP ANTENNAS

D. H. Werner

The Pennsylvania State University
Department of Electrical Engineering
211A Electrical Engineering East
University Park, PA 16802

1. INTRODUCTION

Several useful mathematically exact representations have been developed for the electromagnetic fields radiated by a uniform current circular loop antenna [1–4]. A more general methodology for evaluating the complicated near-field integrals associated with circular loop antennas has been recently introduced in [5]. The main advantages of this approach are that it is applicable to loops of any size and with arbitrary current distribution. Thus far, this technique has only been used for the analysis of loop antennas which have a standing-wave current distribution. In this paper, however, we will demonstrate how this exact integration procedure applies not only to the analysis of standing-wave loop antennas, but also to the analysis of traveling-wave loop antennas.

Previous investigations of traveling-wave loop antennas have focused on the derivation of far-field representations and are only special cases of the analysis presented in this paper. For example, far-field expressions have been found in [6–8] for a single turn traveling-wave loop

where the total change in phase over one complete revolution around the loop is an integer multiple of 2π. This analysis was later extended in [9] to include the more general case of a loop with a traveling-wave current distribution of the form

$$I(\phi) = I_0 e^{-j\gamma\phi} \tag{1}$$

where the parameter γ can in general be complex with a negative imaginary part. In this case, the phase changes over one complete revolution by an amount equal to $2\pi\Re(\gamma)$ radians.

Exact series representations are derived in Section 2 for the near-zone vector potential and corresponding magnetic field components for a traveling-wave loop antenna with a current distribution of the form defined in (1). Convenient far-zone approximations are derived in Section 3 by using the exact near-zone expansions as a starting point. Finally, the exact representations derived in Section 2 are used in Section 4 to investigate how the magnetic fields behave in close proximity to a traveling-wave circular loop antenna.

2. THEORETICAL DEVELOPMENT

The geometry for the standard circular loop antenna of radius a is illustrated in Figure 1. The source point and the field point are designated by the spherical coordinates $(r' = a,\ \theta' = 90^\circ,\ \phi')$ and (r, θ, ϕ), respectively. Hence, the distance from the source point on the loop to the field point at some arbitrary location in space is

$$R' = \sqrt{R^2 - 2ar\sin\theta\cos(\phi - \phi')} \tag{2}$$

where

$$R = \sqrt{r^2 + a^2} \tag{3}$$

If the current distribution is assumed to vary around the loop, i.e., $I(\phi)$, then the vector potential may be expressed in the general form [10]

$$\vec{A} = A_r(r,\theta,\phi)\hat{r} + A_\theta(r,\theta,\phi)\hat{\theta} + A_\phi(r,\theta,\phi)\hat{\phi} \tag{4}$$

where

$$A_r(r,\theta,\phi) = \frac{\mu a \sin\theta}{4\pi}\int_0^{2\pi} I(\phi')\sin(\phi - \phi')\frac{e^{-j\beta R'}}{R'}d\phi' \tag{5}$$

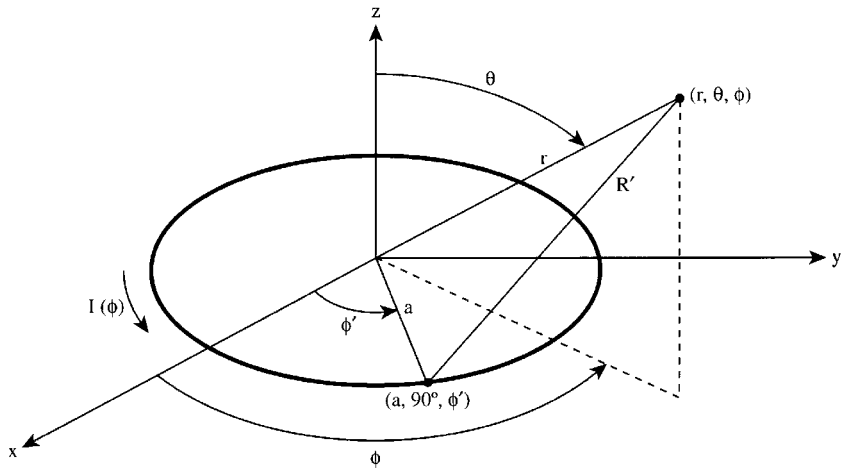

Figure 1. Circular loop antenna geometry.

$$A_\theta(r,\theta,\phi) = \frac{\mu a \cos\theta}{4\pi} \int_0^{2\pi} I(\phi') \sin(\phi - \phi') \frac{e^{-j\beta R'}}{R'} d\phi' \tag{6}$$

$$A_\phi(r,\theta,\phi) = \frac{\mu a}{4\pi} \int_0^{2\pi} I(\phi') \cos(\phi - \phi') \frac{e^{-j\beta R'}}{R'} d\phi' \tag{7}$$

At this point we make use of the technique introduced in [5] in order to transform (5–7) into

$$A_r(r,\theta,\phi) = -\frac{\mu}{2j\beta r} \sum_{m=1}^{\infty} G'_m(\phi) \frac{\left(\beta^2 ar \sin\theta\right)^m}{m!} \frac{h^{(2)}_{m-1}(\beta R)}{(\beta R)^{m-1}} \tag{8}$$

$$A_\theta(r,\theta,\phi) = -\frac{\mu \cot\theta}{2j\beta r} \sum_{m=1}^{\infty} G'_m(\phi) \frac{\left(\beta^2 ar \sin\theta\right)^m}{m!} \frac{h^{(2)}_{m-1}(\beta R)}{(\beta R)^{m-1}} \tag{9}$$

$$A_\phi(r,\theta,\phi) = \frac{\mu\beta a}{2j} \sum_{m=1}^{\infty} G_m(\phi) \frac{\left(\beta^2 ar \sin\theta\right)^{m-1}}{(m-1)!} \frac{h^{(2)}_{m-1}(\beta R)}{(\beta R)^{m-1}} \tag{10}$$

where $\beta = \omega/c = 2\pi/\lambda$, $h^{(2)}_m(x)$ are spherical Hankel functions of the

second kind of order m, and

$$G_m(\phi) = \frac{1}{2\pi} \int_0^{2\pi} I(\phi') \cos^m(\phi - \phi') d\phi' \tag{11}$$

$$G'_m(\phi) = \frac{d}{d\phi} G_m(\phi) \tag{12}$$

This suggests that an exact representation for the three vector potential components may be obtained from (8–10) provided closed-form solutions to the family of integrals given in (11) exist for a particular loop current distribution. Fortunately, it is possible to evaluate these integrals analytically for the majority of commonly assumed current distributions. Finally, once exact representations for the vector potential have been found using (8–12), it is a straightforward procedure to derive the corresponding exact expressions for the electric and magnetic fields via the following well-known relationships:

$$\vec{H} = \frac{1}{\mu} \vec{\nabla} \times \vec{A} \tag{13}$$

$$\vec{E} = \frac{1}{j\omega\varepsilon} \vec{\nabla} \times \vec{H} = \frac{1}{j\omega\mu\varepsilon} \left[\vec{\nabla} \left(\vec{\nabla} \cdot \vec{A} \right) + \beta^2 \vec{A} \right] \tag{14}$$

The first step in the process of obtaining exact near-zone representations for the vector potential components of the traveling-wave loop antenna is to evaluate the integral

$$G_m(\phi) = \frac{I_0}{2\pi} \int_0^{2\pi} e^{-j\gamma\phi'} \cos^m(\phi - \phi') d\phi' \tag{15}$$

which results from substituting (1) into (11). It may be shown that this integral has the following closed-form solution [11]:

$$G_{2n}(\phi) = I_0 e^{-j\gamma\pi} \mathrm{sinc}(\gamma\pi) \left\{ \frac{1}{2^{2n}} \binom{2n}{n} + \frac{1}{2^{2n-1}} \sum_{k=1}^{n} \binom{2n}{n-k} \times \frac{\gamma}{(2k)^2 - \gamma^2} \left[j(2k) \sin(2k)\phi - \gamma \cos(2k)\phi \right] \right\} \tag{16}$$

when m is even (i.e., $m = 2n$) and

$$G_{2n+1}(\phi) = I_0 e^{-j\gamma\pi}\mathrm{sinc}(\gamma\pi) \times \frac{1}{2^{2n}} \sum_{k=0}^{n} \binom{2n+1}{n-k} \frac{\gamma}{(2k+1)^2 - \gamma^2} \times [j(2k+1)\sin(2k+1)\phi - \gamma\cos(2k+1)\phi] \tag{17}$$

when m is odd (i.e., $m = 2n+1$). The function $\mathrm{sinc}(x)$ which appears in (16) and (17) is defined as

$$\mathrm{sinc}(x) = \frac{\sin(x)}{x} \tag{18}$$

Taking the derivative with respect to ϕ of both sides of (16) and (17) yields

$$G'_{2n}(\phi) = I_0 e^{-j\gamma\pi}\mathrm{sinc}(\gamma\pi) \times \frac{1}{2^{2n-1}} \sum_{k=1}^{n} \binom{2n}{n-k} \frac{\gamma(2k)}{(2k)^2 - \gamma^2} \times [j(2k)\cos(2k)\phi + \gamma\sin(2k)\phi] \tag{19}$$

and

$$G'_{2n+1}(\phi) = I_0 e^{-j\gamma\pi}\mathrm{sinc}(\gamma\pi) \times \frac{1}{2^{2n}} \sum_{k=0}^{n} \binom{2n+1}{n-k} \frac{\gamma(2k+1)}{(2k+1)^2 - \gamma^2} \times [j(2k+1)\cos(2k+1)\phi + \gamma\sin(2k+1)\phi] \tag{20}$$

We next recognize the fact that (8–10) may be written as

$$A_r(r,\theta,\phi) = \frac{j\mu}{2\beta r} \left\{ \sum_{n=0}^{\infty} G'_{2n+1}(\phi) \frac{\left(\beta^2 ar\sin\theta\right)^{2n+1}}{(2n+1)!} \frac{h_{2n}^{(2)}(\beta R)}{(\beta R)^{2n}} + \sum_{n=1}^{\infty} G'_{2n}(\phi) \frac{\left(\beta^2 ar\sin\theta\right)^{2n}}{(2n)!} \frac{h_{2n-1}^{(2)}(\beta R)}{(\beta R)^{2n-1}} \right\} \tag{21}$$

$$A_\theta(r,\theta,\phi) = \cot\theta A_r(r,\theta,\phi) \tag{22}$$

$$A_\phi(r,\theta,\phi) = \frac{\mu\beta a}{2j} \left\{ \sum_{n=0}^{\infty} G_{2n+1}(\phi) \frac{\left(\beta^2 ar\sin\theta\right)^{2n}}{(2n)!} \frac{h_{2n}^{(2)}(\beta R)}{(\beta R)^{2n}} + \sum_{n=1}^{\infty} G_{2n}(\phi) \frac{\left(\beta^2 ar\sin\theta\right)^{2n-1}}{(2n-1)!} \frac{h_{2n-1}^{(2)}(\beta R)}{(\beta R)^{2n-1}} \right\} \tag{23}$$

Substituting (19) and (20) into (21) leads to an exact series representation for $A_r(\cdot)$ given by

$$\begin{aligned} A_r(r,\theta,\phi) = {} & \frac{j\mu I_0}{\beta r} e^{-j\gamma\pi}\mathrm{sinc}(\gamma\pi) \\ & \times \left\{ \sum_{n=0}^{\infty}\sum_{k=0}^{n} \frac{\gamma(2k+1)}{(2k+1)^2-\gamma^2} \frac{\left[\left(\beta^2 ar\sin\theta\right)/2\right]^{2n+1}}{(n-k)!(n+k+1)!} \frac{h_{2n}^{(2)}(\beta R)}{(\beta R)^{2n}} \right. \\ & \times [j(2k+1)\cos(2k+1)\phi + \gamma\sin(2k+1)\phi] \\ & + \sum_{n=1}^{\infty}\sum_{k=1}^{n} \frac{\gamma(2k)}{(2k)^2-\gamma^2} \frac{\left[\left(\beta^2 ar\sin\theta\right)/2\right]^{2n}}{(n-k)!(n+k)!} \frac{h_{2n-1}^{(2)}(\beta R)}{(\beta R)^{2n-1}} \\ & \left. \times [j(2k)\cos(2k)\phi + \gamma\sin(2k)\phi] \right\} \end{aligned} \tag{24}$$

Likewise, (16) and (17) may be substituted into (23) in order to arrive at a series expansion for $A_\phi(\cdot)$ which has the form

$$\begin{aligned} A_\phi(r,\theta,\phi) = {} & \frac{\mu\beta a I_0}{2j} e^{-j\gamma\pi}\mathrm{sinc}(\gamma\pi) \\ & \times \left\{ \sum_{n=1}^{\infty} \frac{\left[\left(\beta^2 ar\sin\theta\right)/2\right]^{2n-1}}{n!(n-1)!} \frac{h_{2n-1}^{(2)}(\beta R)}{(\beta R)^{2n-1}} \right. \\ & + \sum_{n=0}^{\infty}\sum_{k=0}^{n} \frac{\gamma(2n+1)}{(2k+1)^2-\gamma^2} \frac{\left[\left(\beta^2 ar\sin\theta\right)/2\right]^{2n}}{(n-k)!(n+k+1)!} \frac{h_{2n}^{(2)}(\beta R)}{(\beta R)^{2n}} \\ & \times [j(2k+1)\sin(2k+1)\phi - \gamma\cos(2k+1)\phi] \\ & + \sum_{n=1}^{\infty}\sum_{k=1}^{n} \frac{\gamma(2n)}{(2k)^2-\gamma^2} \frac{\left[\left(\beta^2 ar\sin\theta\right)/2\right]^{2n-1}}{(n-k)!(n+k)!} \frac{h_{2n-1}^{(2)}(\beta R)}{(\beta R)^{2n-1}} \\ & \left. \times [j(2k)\sin(2k)\phi - \gamma\cos(2k)\phi] \right\} \end{aligned} \tag{25}$$

Substituting the appropriate expansions from (24), (22), and (25) into (13) and performing the required mathematical operations may be shown to result in the following exact near-zone representations for the magnetic field components of the traveling-wave loop:

$$
\begin{aligned}
H_r(r,\theta,\phi) = {} & \frac{\beta(\beta a)^2 I_0 \cos\theta}{4j} e^{-j\gamma\pi}\mathrm{sinc}(\gamma\pi) \\
& \times \left\{ 2\sum_{n=1}^{\infty} \frac{\left[\left(\beta^2 ar\sin\theta\right)/2\right]^{2n-2}}{[(n-1)!]^2} \frac{h_{2n-1}^{(2)}(\beta R)}{(\beta R)^{2n-1}} \right. \\
& + \gamma \sum_{n=0}^{\infty}\sum_{k=0}^{n} \left[\frac{(2k+1)^2-(2n+1)^2}{(2k+1)^2-\gamma^2} \right] \\
& \times \frac{\left[\left(\beta^2 ar\sin\theta\right)/2\right]^{2n-1}}{(n-k)!(n+k+1)!} \frac{h_{2n}^{(2)}(\beta R)}{(\beta R)^{2n}} \\
& \times [\gamma\cos(2k+1)\phi - j(2k+1)\sin(2k+1)\phi] \\
& + \gamma \sum_{n=1}^{\infty}\sum_{k=1}^{n} \left[\frac{(2k)^2-(2n)^2}{(2k)^2-\gamma^2} \right] \\
& \times \frac{\left[\left(\beta^2 ar\sin\theta\right)/2\right]^{2n-2}}{(n-k)!(n+k)!} \frac{h_{2n-1}^{(2)}(\beta R)}{(\beta R)^{2n-1}} \\
& \left. \times [\gamma\cos(2k)\phi - j(2k)\sin(2k)\phi] \right\} \qquad (26)
\end{aligned}
$$

$$
\begin{aligned}
H_\theta(r,\theta,\phi) = {} & \frac{j\beta(\beta a) I_0}{4\beta r} e^{-j\gamma\pi}\mathrm{sinc}(\gamma\pi) \\
& \times \left\{ \gamma^2 \sum_{n=1}^{\infty} \frac{\left[\left(\beta^2 ar\sin\theta\right)/2\right]^{2n-1}}{(n!)^2} \Lambda_{2n}^{0}(R) \right. \\
& - 2\gamma \sum_{n=0}^{\infty}\sum_{k=0}^{n} \frac{\left[\left(\beta^2 ar\sin\theta\right)/2\right]^{2n}}{(n-k)!(n+k+1)!} \Lambda_{2n+1}^{2k+1}(R) \\
& \times [j(2k+1)\sin(2k+1)\phi - \gamma\cos(2k+1)\phi] \\
& - 2\gamma \sum_{n=1}^{\infty}\sum_{k=1}^{n} \frac{\left[\left(\beta^2 ar\sin\theta\right)/2\right]^{2n-1}}{(n-k)!(n+k)!} \Lambda_{2n}^{2k}(R) \\
& \left. \times [j(2k)\sin(2k)\phi - \gamma\cos(2k)\phi] \right\} \qquad (27)
\end{aligned}
$$

$$
\begin{aligned}
H_\phi(r,\theta,\phi) = \frac{\beta(\beta a)(\beta r) I_0 \cos\theta}{2j} e^{-j\gamma\pi} \mathrm{sinc}(\gamma\pi) \\
&\times \left\{ \gamma \sum_{n=0}^{\infty} \sum_{k=0}^{n} \left[\frac{(2k+1)}{(2k+1)^2 - \gamma^2} \right] \right. \\
&\times \frac{\left[\left(\beta^2 a r \sin\theta\right)/2 \right]^{2n}}{(n-k)!(n+k+1)!} \frac{h_{2n+1}^{(2)}(\beta R)}{(\beta R)^{2n+1}} \\
&\times \left[j(2k+1)\cos(2k+1)\phi + \gamma \sin(2k+1)\phi \right] \\
&+ \gamma \sum_{n=1}^{\infty} \sum_{k=1}^{n} \left[\frac{(2k)}{(2k)^2 - \gamma^2} \right] \\
&\times \frac{\left[\left(\beta^2 a r \sin\theta\right)/2 \right]^{2n-1}}{(n-k)!(n+k)!} \frac{h_{2n}^{(2)}(\beta R)}{(\beta R)^{2n}} \\
&\times \left. \left[j(2k)\cos(2k)\phi + \gamma \sin(2k)\phi \right] \right\}
\end{aligned}
\tag{28}
$$

where

$$
\Lambda_n^k(R) = \left[\frac{k^2 - n^2}{k^2 - \gamma^2} \right] \frac{h_{n-1}^{(2)}(\beta R)}{(\beta R)^{n-1}} + (\beta r)^2 \left[\frac{n}{k^2 - \gamma^2} \right] \frac{h_n^{(2)}(\beta R)}{(\beta R)^n} \tag{29}
$$

3. FAR-ZONE APROXIMATIONS

An asymptotic evaluation of the exact series representations for $A_\theta(\cdot)$ and $A_\phi(\cdot)$ can be performed in order to derive useful far-zone approximations. In the far-zone of the loop $r \gg a$ and $R \approx r$, which implies that

$$
\frac{h_{2n}^{(2)}(\beta R)}{(\beta R)^{2n}} \sim j(-1)^n \frac{e^{-j\beta r}}{(\beta r)^{2n+1}} \quad \text{as} \quad \beta r \to \infty \tag{30}
$$

$$
\frac{h_{2n-1}^{(2)}(\beta R)}{(\beta R)^{2n-1}} \sim (-1)^n \frac{e^{-j\beta r}}{(\beta r)^{2n}} \quad \text{as} \quad \beta r \to \infty \tag{31}
$$

These asymptotic expansions may be applied directly to (22), (24) and (25) which leads to the desired set of far-zone approximations given by

$$A_\theta(r,\theta,\phi) \sim j\mu(\beta a) I_0 \cos\theta e^{-j\gamma\pi}\mathrm{sinc}(\gamma\pi)\frac{e^{-j\beta r}}{\beta r} \times \sum_{k=1}^{\infty} \frac{\gamma k}{k^2-\gamma^2}(j)^k \left[jk\cos(k\phi)+\gamma\sin(k\phi)\right] \times \frac{J_k(w)}{w} \quad \text{as} \quad \beta r \to \infty \tag{32}$$

$$A_\phi(r,\theta,\phi) \sim \frac{\mu(\beta a) I_0}{2j} e^{-j\gamma\pi}\mathrm{sinc}(\gamma\pi)\frac{e^{-j\beta r}}{\beta r} \times \left\{ -J_1(w) + 2\sum_{k=1}^{\infty} \frac{\gamma}{k^2-\gamma^2}(j)^k \times \left[jk\sin(k\phi)-\gamma\cos(k\phi)\right] J_k'(w) \right\} \quad \text{as} \quad \beta r \to \infty \tag{33}$$

where $J_k(x)$ are cylindrical Bessel functions of the first kind of order k and

$$w = \beta a \sin\theta \tag{34}$$

The corresponding far-zone approximations for the nontrivial electromagnetic field components of the traveling-wave loop are then

$$H_\theta(r,\theta,\phi) \approx \frac{\beta a I_0}{2} e^{-j\gamma\pi}\mathrm{sinc}(\gamma\pi)\frac{e^{-j\beta r}}{r} \times \left\{ -J_1(w) + 2\sum_{k=1}^{\infty} \frac{\gamma}{k^2-\gamma^2}(j)^k \times \left[jk\sin(k\phi)-\gamma\cos(k\phi)\right] J_k'(w) \right\} \tag{35}$$

$$H_\phi(r,\theta,\phi) \approx \beta a I_0 \cos\theta e^{-j\gamma\pi}\mathrm{sinc}(\gamma\pi)\frac{e^{-j\beta r}}{r} \times \sum_{k=1}^{\infty} \frac{\gamma k}{k^2-\gamma^2}(j)^k \times \left[jk\cos(k\phi)+\gamma\sin(k\phi)\right]\frac{J_k(w)}{w} \tag{36}$$

$$E_\theta(r,\theta,\phi) \approx \eta\beta a I_0 \cos\theta e^{-j\gamma\pi}\mathrm{sinc}(\gamma\pi)\frac{e^{-j\beta r}}{r} \times \sum_{k=1}^{\infty} \frac{\gamma k}{k^2-\gamma^2}(j)^k \times \left[jk\cos(k\phi)+\gamma\sin(k\phi)\right]\frac{J_k(w)}{w} \tag{37}$$

$$E_\phi(r,\theta,\phi) \approx -\frac{\eta\beta a I_0}{2} e^{-j\gamma\pi}\mathrm{sinc}(\gamma\pi)\frac{e^{-j\beta r}}{r} \times \left\{ -J_1(w) + 2\sum_{k=1}^{\infty} \frac{\gamma}{k^2-\gamma^2}(j)^k \times \left[jk\sin(k\phi) - \gamma\cos(k\phi) \right] J_k'(w) \right\} \quad (38)$$

which are in agreement with the results previously reported in [9].

4. RESULTS

There are several advantages and useful applications of the mathematically exact near-field expansions for the traveling-wave loop given in (26–28). For instance, they can be used to gain additional insight into the problem physics as well as provide general expressions which contain all of the classical approximations as special cases. These series expansions were implemented on a computer in order to investigate the near-zone magnetic field behavior of a traveling-wave loop antenna. Figure 2 contains plots of the total magnetic field intensity as a function of ϕ for various values of the parameter γ. The loop current and radius were assumed to be $I_0 = 1A$ and $a = \lambda/2\pi(\beta a = 1)$, respectively, with field point coordinates of $\theta = 90^\circ$ and $r = \lambda/2(\beta r = \pi)$. This set of curves demonstrates how the magnetic field intensity varies in the horizontal plane of the loop $(\theta = 90^\circ)$ for noninteger values of γ. Similar plots are shown in Fig. 3 which illustrate the variations in field intensity produced in the vertical plane of the loop (i.e., $\phi = 90^\circ$ and $0^\circ \leq \theta \leq 360^\circ$). Finally, the curves shown in Fig. 4 document the behavior of the magnetic field intensity as r varies between $\lambda/4$ and $3\lambda/4$ with $\theta = 90^\circ$ and $\phi = 90^\circ$.

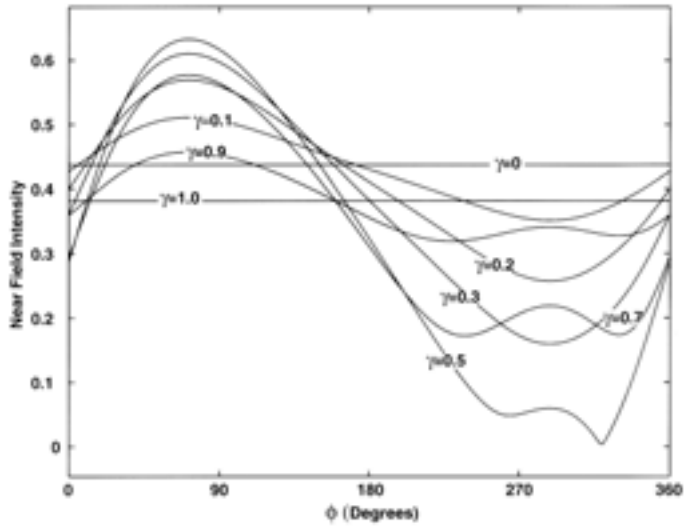

Figure 2. Total near-zone magnetic field intensity in A/m as a function of ϕ for several different values of the parameter γ. In this case $I_0 = 1\,A,\ a = \lambda/2\pi(\beta a = 1),\ \theta = 90^\circ$ and $r = \lambda/2(\beta r = \pi)$.

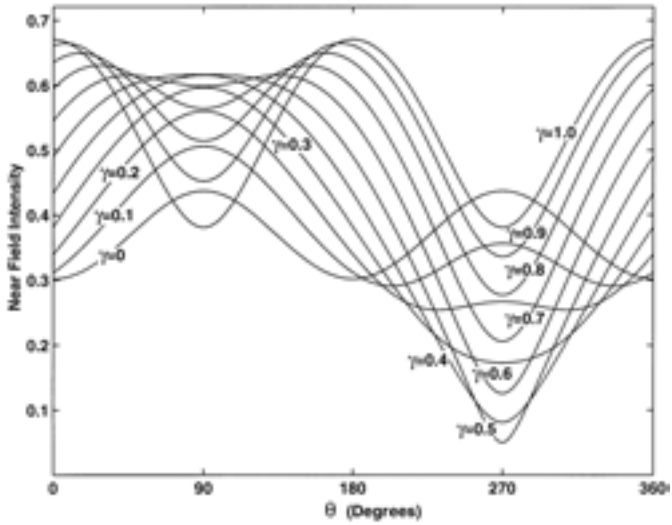

Figure 3. Total near-zone magnetic field intensity in A/m as a function of θ for several different values of the parameter γ. In this case $I_0 = 1\,A,\ a = \lambda/2\pi(\beta a = 1),\ \phi = 90^\circ,$ and $r = \lambda/2(\beta r = \pi)$.

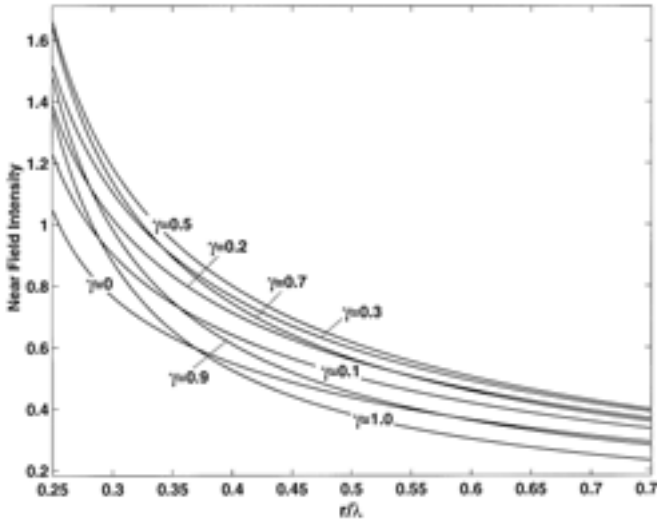

Figure 4. Total near-zone magnetic field intensity in A/m as a function of r for several different values of the parameter γ. In this case $I_0 = 1\,A,\ a = \lambda/2\pi(\beta a = 1),\ \theta = 90°,$ and $\phi = 90°$.

5. CONCLUSIONS

An exact integration procedure for vector potentials of thin traveling-wave circular loop antennas has been introduced in this paper. The technique is straightforward to apply and leads to general series representations which are valid not only in the far-field of the loop, but also in its near-field region. Finally, asymptotic methods were applied to these exact series representations in order to find a useful set of far-field approximations.

ACKNOWLEDGMENT

The author would like to thank Matthew K. Emsley for his assistance with the preparation of Figures 2–4.

REFERENCES

1. Greene, F. M., "The near-zone magnetic field of a small circular loop antenna," *J. Res. NBS,* 71-C(4), 319–326, 1967.
2. Werner, D. H., "Analytical and numerical methods for evaluating electromagnetic field integrals associated with current-carrying wire antennas," *Advanced Electromagnetism: Foundations, Theory and Applications,* edited by T. W. Barrett and D. M. Grimes, 682–762, World Scientific, Singapore, 1995.
3. Overfelt, P. L., "Near-fields of a constant current thin circular loop antenna of arbitrary radius," *IEEE Trans. Antennas Propagat.,* 44(2), 166–171, 1996.
4. Werner, D. H., and T. W. Colegrove, "On a new cylindrical harmonic representation for spherical waves," *IEEE Trans. Antennas Propagat.,* 47(1), 97–100, 1999.

5. Werner, D. H., "An exact integration procedure for vector potentials of thin circular loop antennas," *IEEE Trans. Antennas Propagat.,* 44(2), 157–165, 1996.
6. Sherman, J. B., "Circular loop antennas at ultra-high frequencies," *Proc. IRE,* 32, 534–537, 1944.
7. Knudsen, H. L., "The field radiated by ring quasi-array of an infinite number of tangential or radial dipoles," *Proc. IRE,* 41, 781–789, 1953.
8. Adekola, S. A., "On the excitation of a circular loop antenna by traveling- and standing-wave current distributions," *Int. J. Electronics,* 54(6), 705–732, 1983.
9. Prasad, S. M., and B. N. Das, "A circular loop antenna with traveling-wave current distribution," *IEEE Trans. Antennas Propagat.,* AP-18(2), 278–280, 1970.
10. Balanis, C. A., *Antenna Theory, Analysis, and Design,* Harper & Row, New York, 1982.
11. Gradshteyn, I. S., and I. M. Ryzhik, *Table of Integrals, Series, and Products,* Academic Press, Inc., 1994.